

1 **Detailed Methods**

2 **Subjects and Experimental Design**

3 This is a cross-sectional, case-control study. De-identified samples and subject  
4 information were acquired from the Maternal Fetal Tissue Bank of the Women's Health  
5 Tissue Repository at the University of Iowa<sup>1</sup>. Tissue bank inclusion and exclusion  
6 criteria have been previously published<sup>1</sup>. The Maternal Fetal Tissue Bank has been  
7 approved by the Institutional Review Board of the University of Iowa (IRB#200910784).  
8 Details about sample collection for the tissue bank are published elsewhere<sup>1</sup>. The  
9 present study was reviewed by the Institutional Review Board of the University of North  
10 Texas Health Science Center, which determined the protocol to meet criteria for exempt  
11 status (IRB#2017-065, exempt category 4).

12 Cases consisted of 19 pregnant women clinically diagnosed with preeclampsia.  
13 Nineteen healthy pregnant controls were matched to cases for gestational age at  
14 sampling. Subject characteristics can be found in Table S1. Maternal blood was  
15 collected in the third trimester (28-41 weeks of gestation) during routine venipuncture.  
16 Blood was collected into ACD-A tubes (Becton Dickinson) containing: 22.0 g/L trisodium  
17 citrate, 8.0 g/L citric acid, and 24.5 g/L dextrose, and stored in 4°C until further  
18 processing. Blood was then separated into plasma and peripheral blood mononuclear  
19 cells (PBMCs). PBMCs were stored in cryopreservation media (RPMI media [40% v/v],  
20 FBS [50%], and DMSO [10%]). Plasma samples were snap frozen and stored at -80°C  
21 and PBMCs were snap frozen and maintained in liquid nitrogen.

22

23

## 24 **DNA Measurements – Absolute quantification polymerase chain reaction (qPCR)**

25 DNA was isolated and quantified as published previously<sup>2</sup>, with a few  
26 modifications. Briefly, DNA from plasma and PBMCs (200  $\mu$ L) was isolated using a  
27 magnetic bead-based extraction method (Omega Bio-tek) with a final elution volume of  
28 360  $\mu$ L. DNA from plasma samples was isolated in the presence and absence of lysis  
29 buffer to elucidate the contribution of the membrane bound component of plasma, as  
30 this has been noted previously to contain mtDNA<sup>3, 4</sup>.

31 TaqMan<sup>TM</sup> chemistry-based absolute quantification of nuclear DNA (nDNA) and  
32 mtDNA are detailed elsewhere<sup>2</sup>. Briefly, isolated nDNA (2  $\mu$ L) was quantified on a 7500  
33 Real-Time PCR System (Applied Biosystems) using the Quantifiler<sup>TM</sup> Trio DNA  
34 Quantification Kit (Applied Biosystems, Waltham, MA, USA; Cat. No. 4482910) in 18  $\mu$ L  
35 of master-mix for a total reaction volume of 20  $\mu$ L. PCR settings were as follows: 95 °C  
36 for 2 minutes and 40 cycles of 95 °C for 9 seconds with 60°C at 30 seconds. Cycle  
37 threshold ( $C_T$ ) was compared to five 1:10 serial dilutions of male, genomic reference  
38 DNA in order to calculate a concentration [ $nDNA/\mu L_{DNA\ isolate}$ ] according to the  
39 manufacturer's directions.

40 Isolated mtDNA was quantified using a method modified from Kavlick et al.<sup>5</sup> and  
41 detailed previously<sup>2</sup>. The target sequence for this analysis is the *MT-ND5* gene  
42 (mitochondrial NADH:ubiquinone oxidoreductase core subunit 5; GenBank Gene ID:  
43 4540), spanning positions 13,288-12,392 of the mitochondrial genome (based on  
44 revised Cambridge Reference Sequence positions)<sup>6</sup>. Isolated mtDNA (2  $\mu$ L) was added  
45 to 23  $\mu$ L of master-mix for a total reaction volume of 25  $\mu$ L. Quantification was  
46 performed on a 7500 Real-Time PCR System (Applied Biosystems), with the following

47 settings: 9600 emulation, 50 °C for 2 minutes, 95 °C for 10 minutes, and 40 cycles of 95  
 48 °C for 15 seconds with 60 °C for 1 minute.  $C_T$  of samples was compared to eight, 1:10,  
 49 serial dilutions of double-stranded, synthetic, reference DNA (gBlocks® gene fragment;  
 50 Integrated DNA Technologies, Coralville, IA, USA) in order to calculate a concentration  
 51 of mtDNA in the isolate [ $mtDNA/\mu L_{DNA\ isolate}$ ]. The qPCR primers, probes, and synthetic  
 52 DNA standards employed for mtDNA analysis are detailed in Table S2.

53 For DNA quantification, amplification efficiency >80% and  $R^2$  >99% was  
 54 considered adequate. Concentration of plasma DNA ( $[DNA]^{plasma}$ ) was determined by  
 55 relating the calculated concentration of the DNA lysate ( $[DNA]^{isolate}$ ) multiplied by the  
 56 volume of elution buffer (0.360 mL) to the known volume of isolated plasma (0.200 mL)  
 57 (equation 1a-b), and it was expressed as picograms (pg) per mL of plasma. Total DNA  
 58 was calculated as the sum of mtDNA and nDNA, in pg/mL plasma.

$$59 \quad [DNA]^{plasma} \text{ pg/mL} \times 0.2 \text{ mL} = [DNA]^{isolate} \text{ pg/mL} \times 0.36 \text{ mL} \quad (1a)$$

$$60 \quad [DNA]^{plasma} \text{ pg/mL} = \frac{0.36 \text{ mL} \times [DNA]^{isolate} \text{ pg/mL}}{0.2 \text{ mL}} \quad (1b)$$

61 The DNA content of PBMCs is presented as cellular equivalents (Ceq) per microliter  
 62 DNA isolate [ $pg/\mu L_{DNA\ isolate}$ ] for nDNA and as mtDNA genome copies per Ceq. Ceq was  
 63 calculated based on the estimated molecular weight of nDNA per human diploid cell of  
 64 6.7pg (equation 2a). mtDNA copies were calculated by relating number of mitochondrial  
 65 genomes that has a mass of 1 pg, where 1 pg is equal to 58,800 mitochondrial genome  
 66 copies (equation 2b).

$$67 \quad Ceq^{PBMC}/\mu L = [nDNA]^{PBMC} \text{ pg}/\mu L \times \frac{1 \text{ Ceq}}{6.7 \text{ pg}} \quad (2a)$$

$$68 \quad [mtDNA]^{PBMC} \text{ copies}/\mu L = [mtDNA]^{PBMC} \text{ pg}/\mu L \times \frac{58,800 \text{ copies}}{1 \text{ pg}} \quad (2b)$$

69 **DNase I measurement in maternal plasma**

70 DNase I concentrations in maternal plasma were measured using an ELISA  
71 (MyBioSource, Ca MBS763541). Plasma samples were diluted 1:10 before performing  
72 the ELISA per manufacturer's instructions.

73

74 **TLR-9 stimulation**

75 To determine the immunostimulatory potency of plasma from pregnancies with  
76 preeclampsia in relation to TLR-9 activation, we used an engineered cell line of human  
77 embryonic kidney (HEK) 293 cells transfected with a human *TLR-9* gene (HEK-Blue™  
78 hTLR-9 cells, Invivogen). HEK-Blue™ hTLR-9 cells express an inducible secreted  
79 embryonic alkaline phosphatase (SEAP) reporter gene under the control of a fused  
80 promoter containing NF-κB and AP-1 binding sites. Stimulation of HEK-Blue™ hTLR-9  
81 cells with a TLR-9 ligand activates NF-κB and AP-1, which induce the production of  
82 SEAP. HEK-Blue™ hTLR-9 cells were cultured and maintained according to the  
83 manufacturer's instructions. TLR-9 stimulation was assessed in response to 10%  
84 plasma from women with healthy pregnancies or pregnancies complicated by  
85 preeclampsia by monitoring SEAP production in a cell-culture detection medium (HEK-  
86 Blue™ Detection, Invivogen). TLR-9 agonists (ODN 2006 and ODN 2395, Invivogen)  
87 and antagonist (ODN 2088, Invivogen) were used as positive and negative controls of  
88 SEAP production, respectively. After 24 hours of incubation, SEAP production was  
89 quantified by reading the optical density of samples at 630 nm using a BioTEK Synergy  
90 HTX spectrophotometer.

91

## 92 **Data Analysis and Statistics**

93 To identify the most important patient characteristics associated with the  
94 outcome of preeclampsia, bootstrapped penalized logistic regression was implemented.  
95 All elements of regression analyses were carried out in R software version 4.0.2<sup>7</sup>. The  
96 following penalized regression models were fit and their performances compared to  
97 select the best model: 1) least absolute shrinkage and selection operator (LASSO)  
98 regression; 2) ridge regression; and 3) elastic net regression. These models perform  
99 optimally under different conditions: LASSO performs best when few predictors  
100 influence the outcome<sup>8</sup>; ridge performs best when many predictors have a small effect  
101 on the outcome<sup>8, 9</sup>; and elastic net performs best when the dataset is an intermediate  
102 between the two<sup>10</sup>. To adhere to test assumptions of independent observations while  
103 not eliminating potentially important patient characteristics, related characteristics were  
104 grouped *a priori* (Table S3) and an in-house code was developed that selected a single  
105 characteristic from each group to generate all possible combinations of independent  
106 characteristics ( $n = 192$  datasets). Bootstrapped ( $R = 500$ ) 10-fold cross-validation  
107 LASSO, ridge, and elastic net were then performed on each dataset and best model fit  
108 was assigned by lowest prediction error (specifically, lowest median root mean squared  
109 error; RMSE<sup>11, 12</sup>). Predictive accuracy of the final model against a simulated naïve  
110 prediction dataset was assessed by the bootstrap estimate ( $R = 500$ ) of the area under  
111 the curve of the receiver operator characteristic (AUC ROC) with confidence intervals  
112 (CI 95%) calculated from standard error. Characteristics selected by the model at least  
113 75% of the time (variable importance probability; VIP 0.75)<sup>13</sup> for all bootstrap samples  
114 were regarded as most important. Using this approach, the optimized predictor

115 combination and model were thus selected to best explain the association between  
116 patient characteristics and the diagnosis of preeclampsia.

117

## 118 Statistics

119 Statistical analyses were performed using Prism (Version 8, GraphPad, San  
120 Diego, CA, USA). Data distribution was assessed using the D' Agostino-Pearson  
121 omnibus test and the robust regression and outlier removal (ROUT) method was used  
122 to identify and remove outliers. Non-parametric statistics were used for non-normally  
123 distributed data sets. Group differences in DNA quantities and DNase I concentrations  
124 were determined using Student's t-test or Mann-Whitney *U* test. A two-way analysis of  
125 variance (ANOVA) followed by Sidak's post-hoc analysis was used determine the effect  
126 of fetal sex on group differences in DNA quantities. Spearman correlation was applied  
127 to evaluate relationships between DNA quantities and DNase I for each group. DNA  
128 outcomes are presented as mean  $\pm$  standard error of the mean (SEM). Subject  
129 characteristics are presented as mean with minimum and maximum unless otherwise  
130 indicated. Exact P values are presented for each analysis.

131

132

133 **Supplementary Tables**134 **Table S1. Subject characteristics**

	<i>Control</i>	<i>Preeclampsia</i>	<i>P value</i>
	(n = 19)	(n = 19)	
<i>Race (%)</i>			
Caucasian	19 (100)	18 (95)	
Non-Hispanic	19 (100)	19 (100)	
<i>BMI (kg/m<sup>2</sup>)</i>	27 (18, 46)	31 (18, 50)	0.1
Overweight (BMI: 25-29.9) (%)	3 (16)	7 (37)	
Obese (BMI: ≥ 30) (%)	4 (21)	8 (42)	
<i>MAP (mmHg)</i>	90 (76, 101)	108 (86, 129)	<0.0001
SBP (mmHg)	124 (105, 140)	146 (122, 170)	<0.0001
DBP (mmHg)	73 (57, 87)	89 (67, 112)	<0.0001
<i>History of chronic hypertension (%)</i>	0 (0)	8 (42)	
<i>History of preeclampsia (%)</i>	0 (0)	4 (21)	
<i>Medications (%)</i>			
Aspirin	0 (0)	3 (16)	
Magnesium	0 (0)	3 (16)	
Nifedipine	0 (0)	2 (11)	
<i>Gestational age at sample (weeks)</i>	33 (28, 39)	34 (28, 41)	0.7
<i>Gestational age delivery (weeks)</i>	39 (37, 42)	36 (31, 41)	0.0002
<i>Mode of delivery (%)</i>			
NSVD	14 (74)	8 (42)	

VAVD	0 (0)	2 (11)	
Cesarean section	5 (26)	9 (47)	
<i>Neonatal weight (kg)</i>	3.3 (1.5, 4.6)	2.7 (1.5, 3.9)	0.0076
<i>Neonatal sex (F:M)</i>	(12:7)	(7:12)	
<i>Apgar, 1 minute</i>	7.58 (3,9)	7.05 (4, 9)	0.4
<i>Apgar, 5 minutes</i>	8.95 (8, 9)	8.42 (6, 9)	0.028

---

135

136 Maternal BMI, MAP, SBP, DBP, gestational age at delivery, and neonatal weight were  
137 analyzed using unpaired t-test. Gestational age at sample, Apgar (1 minute), and Apgar  
138 (5 minute) were analyzed with Mann-Whitney *U* test. Values presented as mean with  
139 minimum and maximum unless otherwise noted. BMI, body mass index at first obstetric  
140 visit; MAP, mean arterial blood pressure at time of blood sample; SBP, systolic blood  
141 pressure at time of blood sample; DBP, diastolic blood pressure at time of blood  
142 sample; NSVD, normal spontaneous vaginal delivery; VAVD, vacuum-assisted vaginal  
143 delivery.

144



145 **Table S2. Primer, probe, and synthetic standard nucleotide sequences for**  
146 **absolute qPCR of mitochondrial DNA**

---

mtDNA (*MT-ND5*) F: 5'- GGC ATC AAC CAA CCA CAC CTA -3'

mtDNA (*MT-ND5*) R: 5'- ATT GTT AAG GTT GTG GAT GAT GGA -3'

TaqMan probe: 5'- **6FAM** CAT TCC TGC ACA TCT G **MGBNFQ** -3'

SS (gBlock) F: 5'- TG TTC TGT TCA TTG TTA AGG TTG TGG ATG ATG  
GAC CCG GAG CAC ATA AAT AGT CGT TAT TTG AAG  
AAG GCG TGG GTA CAG ATG TGC AGG AAT GCT AGG  
TGT GGT TGG TTG ATG CCG ATT GGA TTG -3'

SS (gBlock) R: 5'- CAA TCC AAT CGG CAT CAA CCA ACC ACA CCT AGC  
ATT CCT GCA CAT CTG TAC CCA CGC CTT CTT CAA ATA  
ACG ACT ATT TAT GTG CTC CGG GTC CAT CAT CCA CAA  
CCT TAA CAA TGA ACA GAA CA -3'

---

147

148 F, forward. R, reverse. *MT-ND5*, mitochondrial NADH:ubiquinone oxidoreductase core  
149 subunit 5. 6FAM, 6-Carboxyfluorescein. MGBNFQ, minor groove binder non-fluorescent  
150 quencher. SS, synthetic standard

**Table S3. Variable groupings used for dataset generation.**

<b>Included in all datasets</b>	<b>Group 2: Neonatal characteristics</b>	<b>Group 4: Extracellular mtDNA</b>
nDNA ng/ml plasma	Neonatal birth length (cm)	<b>signaling</b>
DNase1 ng/ml plasma	Neonatal head circumference (cm)	mtDNA pg/ml plasma (membrane-
Mode of delivery	Gestational age at delivery (days)	bound)
Maternal age at delivery	Neonatal birth weight (g)	mtDNA pg/ml plasma (membrane-
Neonatal sex	Apgar1 score	unbound)
BMI at NOB	Apgar5 score	
<b>Group 1: Maternal blood pressure</b>	<b>Group 3: Maternal reproductive</b>	
Systolic blood pressure (SBP)	<b>history</b>	
Diastolic blood pressure (DBP)	History preeclampsia	
Mean arterial pressure (MAP)	Maternal gravidity	
Chronic hypertension	Maternal parity	
	Number spontaneous abortions	

Datasets were comprised of select variables included in all datasets and one variable randomly chosen from Groups 1-

4. Groupings of related variables determined *a priori*; variables included in all datasets were those that were

---

independent from all other variables in the original dataset. BMI, body mass index; NOB, time of first obstetric appointment.

**Table S4. Coefficients and odds ratios for patient characteristics (elastic net)**

	<b>Coeff</b>	<b>Coeff SE</b>	<b>OR</b>	<b>OR SE</b>	<b>OR CI (95%)</b>
Intercept	-2.5034	0.1410	0.0818	0.0184	(0.0457, 0.1179)
nDNA, ng/ml plasma	0.5032	0.0822	1.6540	0.1110	(1.4365, 1.8716)
mtDNA, pg/ml plasma (membrane-unbound)	-0.0111	0.0013	0.9890	0.00131	(0.9864, 0.9915)
DNase I, ng/ml plasma	0.1617	0.0199	1.1755	0.0221	(1.1322, 1.2188)
BMI	0.0208	0.0015	1.0210	0.0015	(1.018, 1.024)
History preeclampsia (Yes)	0.3710	0.0206	1.4492	0.0281	(1.3941, 1.5043)
Neonatal sex (Male)	0	0.0020	1	0.0020	(0.9961, 1.0039)
Mode delivery (Vaginal)	-0.0584	0.0182	0.9433	0.0174	(0.9092, 0.9774)
Maternal age	0.0132	0.0025	1.0133	0.0026	(1.0083, 1.0183)
Birth weight	-0.0001	7.55e-06	0.9999	7.55e-06	(0.9999, 0.9999)
MAP	0.0222	0.0006	1.0225	0.0006	(1.0214, 1.0236)

Values in parentheses indicate reference state for coefficients and odds ratios. Values are the result of 500 bootstraps.

BMI, body mass index; CI, confidence interval (95%); Coeff, coefficient; MAP, mean arterial pressure; mtDNA, mitochondrial DNA; nDNA, nuclear DNA; OR, odds ratio; SE, standard error

153

154

**Table S5. Model comparison**

	<b>RMSE</b>	<b>SE</b>	<b>CI (95%)</b>
Ridge	0.2627	0.0179	(0.2276, 0.2978)
LASSO	0.3200	0.0193	(0.2822, 0.3578)
Elastic Net	0.2438	0.0196	(0.2054, 0.2823)

RMSE: median root mean square error; SE: standard error; CI: confidence interval (95%)

155

156

157

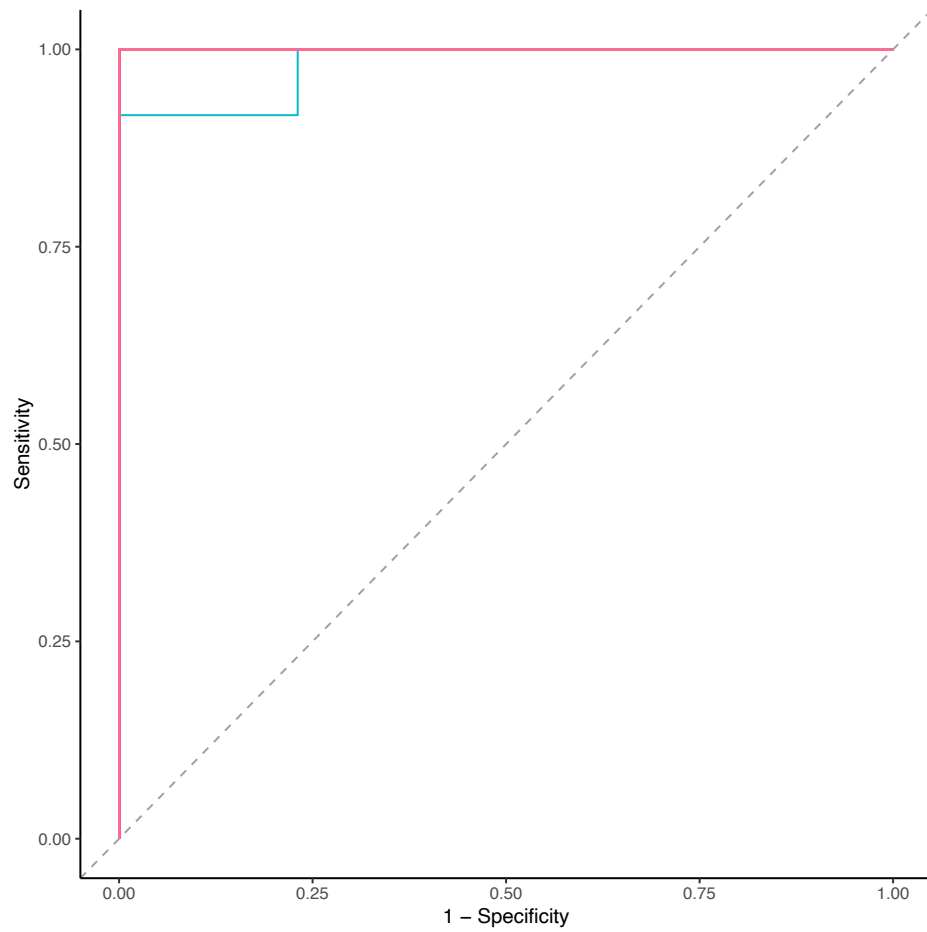
158

**Table S6. Model accuracy and receiver operating characteristic**

	<b>Boot Stat</b>	<b>SE</b>	<b>CI (95%)</b>
Model Accuracy	1	0.0012	(0.9977, 1.0023)
AUC ROC	1	0.0009	(0.9983, 1.0017)

Boot stat: bootstrap summary statistic; SE: standard error; CI: confidence interval (95%); AUC ROC: area under curve of the receiver operating characteristic

160 **Supplementary Figures**



161

162

163 **Figure S1. Accuracy of elastic net penalized regression in the current study. AUC**

164 ROC plot R = 500 simulations (supplementary)



165 **REFERENCES**

- 166 1. Santillan MK, Leslie KK, Hamilton WS, Boese BJ, Ahuja M, Hunter SK and  
167 Santillan DA. Collection of a lifetime: a practical approach to developing a longitudinal  
168 collection of women's healthcare biological samples. *Eur J Obstet Gynecol Reprod Biol.*  
169 2014;179:94-9.
- 170 2. Cushen SC, Sprouse ML, Blessing A, Sun J, Jarvis SS, Okada Y, Fu Q, Romero  
171 SA, Phillips NR and Goulopoulou S. Cell-free mitochondrial DNA increases in maternal  
172 circulation during healthy pregnancy: a prospective, longitudinal study. *Am J Physiol*  
173 *Regul Integr Comp Physiol.* 2020;318:R445-R452.
- 174 3. Keseru JS, Soltesz B, Lukacs J, Marton E, Szilagyi-Bonizs M, Penyige A, Poka R  
175 and Nagy B. Detection of cell-free, exosomal and whole blood mitochondrial DNA copy  
176 number in plasma or whole blood of patients with serous epithelial ovarian cancer. *J*  
177 *Biotechnol.* 2019;298:76-81.
- 178 4. Ye W, Tang X, Liu C, Wen C, Li W and Lyu J. Accurate quantitation of circulating  
179 cell-free mitochondrial DNA in plasma by droplet digital PCR. *Anal Bioanal Chem.*  
180 2017;409:2727-2735.
- 181 5. Kavlick MF, Lawrence HS, Merritt RT, Fisher C, Isenberg A, Robertson JM and  
182 Budowle B. Quantification of human mitochondrial DNA using synthesized DNA  
183 standards. *J Forensic Sci.* 2011;56:1457-63.
- 184 6. Anderson S, Bankier AT, Barrell BG, de Bruijn MH, Coulson AR, Drouin J,  
185 Eperon IC, Nierlich DP, Roe BA, Sanger F, Schreier PH, Smith AJ, Staden R and  
186 Young IG. Sequence and organization of the human mitochondrial genome. *Nature.*  
187 1981;290:457-65.

- 188 7. R: A language and environment for statistical computing. [computer program].  
189 Vienna, Austria: R Foundation for Statistical Computing; 2020.
- 190 8. Tibshirani R. Regression Shrinkage and Selection via the Lasso. *Journal of the*  
191 *Royal Statistical Society Series B (Methodological)*. 1996;58:267-288.
- 192 9. Hoerl AE and Kennard RW. Ridge Regression: Biased Estimation for  
193 Nonorthogonal Problems. *Technometrics*. 2000;42:80-86.
- 194 10. Zou H and Hastie T. Regularization and Variable Selection via the Elastic Net.  
195 *Journal of the Royal Statistical Society Series B (Statistical Methodology)*. 2005;67:301-  
196 320.
- 197 11. Willmott CJ. Some Comments on the Evaluation of Model Performance. *Bulletin*  
198 *of the American Meteorological Society*. 1982;63:1309-1313.
- 199 12. Price DT, McKenney DW, Nalder IA, Hutchinson MF and Kesteven JL. A  
200 comparison of two statistical methods for spatial interpolation of Canadian monthly  
201 mean climate data. *Agricultural and Forest Meteorology*. 2000;101:81-94.
- 202 13. Mills PB, Holtz KA, Szefer E, Noonan VK and Kwon BK. Early predictors of  
203 developing problematic spasticity following traumatic spinal cord injury: A prospective  
204 cohort study. *J Spinal Cord Med*. 2020;43:315-330.

205